Available online at www.sciencedirect.com
ScienceDirect
Journal of Marine Systems 66 (2007) 297–308
JOURNAL OF MARINE SYSTEMS
www.elsevier.com/locate/jmarsys

Surface CO_2 measurements in the English Channel and Southern Bight of North Sea using voluntary observing ships

X.A. Padin *, M. Vázquez-Rodríquez, A.F. Ríos, F.F. Pérez

Instituto de Investigacións Mariñas (CSIC), Eduardo Cabello 6, 36208 Vigo, Spain

Received 12 November 2005; accepted 17 May 2006
Available online 12 September 2006

Abstract

Ships of opportunity have been used to investigate ocean–atmosphere CO_2 fluxes in the English Channel and Southern Bight of the North Sea. Continuous underway measurements of the fugacity of seawater carbon dioxide (fCO_2^{sw}), chlorophyll, temperature and salinity have been performed along 26 transects during the spring and autumn periods. The spatial fCO_2^{sw} distribution along the Channel and Southern Bight is modulated by the photosynthetic activity, temperature changes and water mixing between inputs from the North Atlantic Ocean and riverine discharges. The seasonal variability of fCO_2^{sw} is assessed and discussed in terms of the biology and temperature effects, these having similar impacts. The variation of fCO_2^{sw} shows similar interannual patterns, with lower values in spring. The annual average of air–sea CO_2 fluxes places the English Channel as neutral area of CO_2 uptake. The spring and autumn data allow differentiating between distal and proximal continental areas. The Southern Bight shows a tendency towards net CO_2 uptake on the distal continental shelf, whereas the Scheldt and Thames Plumes show a CO_2 source behaviour on the proximal continental shelves.

Keywords: Carbon dioxide; Air–sea exchange; English Channel; Temporal-spatial variability; Ships of opportunity

1. Introduction

The continental shelves play an important role in the oceanic uptake of atmospheric CO_2, even though it only represents 7% of the total oceanic area (Walsh et al., 1981). The high biological activity of primary producers in the ocean margins, ranging from 15% to 30% of total primary production (Walsh, 1988; Longhurst et al., 1995) causes the intense CO_2 absorption from the atmosphere. Tsunogai et al. (1999) have proposed that the continental shelves may act as a "continental shelf pump" drawing the atmospheric CO_2 into the open ocean.

Recent detailed measurements classified the continental shelves in the middle and high latitudes of the Northern Hemisphere as sinks of atmospheric CO_2. Such is the case of the East China Sea (Chen and Wang, 1999; Wang et al., 2000) and the European shelf (Thomas and Schneider, 1999; Frankignoulle and Borges, 2001; Borges and Frankignoulle, 2002; Thomas et al., 2004). Nevertheless, CO_2 emissions to the atmosphere have been also reported from the United States South Bight (DeGrandpre et al., 2002; Cai et al., 2003), Arabian Sea (Goyet et al., 1998), South Brazil Bight (Ito et al., 2005) and South China Sea (Zhai et al., 2005). The discrepancy in terms of the air–sea CO_2 exchange seems to have a dependency with latitude (Cai and Dai, 2004). The lack of CO_2 measurements in the coastal oceans precludes establishing a classification of the continental shelves in terms of CO_2 as sinks and

* Corresponding author. Tel.: +34 986 231930x377; fax: +34 986 292762.
E-mail address: padin@iim.csic.es (X.A. Padin).

0924-7963/$ - see front matter
doi:10.1016/j.jmarsys.2006.05.011

sources (Fasham et al., 2001). This is especially relevant because a large variety of processes (shelf-edge discontinuities, vertical mixing, upwelling/downwelling, slope currents, sediment remineralization, tidal fronts, river inputs, eutrophication…) takes place in these areas and has an influence on the carbon cycle.

Frankignoulle and Borges (2001) classified the European distal continental shelf as a CO_2 sink with similar uptake capacities compared to other continental shelves (Boehme et al., 1998; Tsunogai et al., 1999). Other studies have described proximal continental shelves as a net source of CO_2 (Smith and Mackenzie, 1987; Frankignoulle et al., 1996; Gattuso et al., 1998; Cai and Wang, 1998; Cai et al., 1999, 2000; Raymond et al., 2000). This apparent controversy can be sorted out by looking at the relative importance of each of the processes involved in the net CO_2 balance along the continental shelf. In this sense, the distal continental shelf is characterized by predominance of organic carbon export (autotrophic). On the contrary, in the proximal continental shelf the terrestrial and anthropogenic inputs (heterotrophic) prevail.

The aim of the present paper is to investigate the spatial and temporal variability of fCO_2^{sw} along the English Channel (EnC) and Southern Bight of the North Sea (SB) from recent data sets obtained using ships of opportunity. The seasonal cycle of fCO_2^{sw} is investigated in relation to the water masses, evaluating the role and relative contribution of biological activity, and temperature in the EnC and SB.

The present work is laid out as follows: we present the spatial and temporal variability of the surface distribution of fCO_2^{sw} in relation with the thermohaline characteristics of the EnC and SB (Section 3.1). Next we investigate the role of biology and temperature effect on the fCO_2^{sw} concentrations (Section 3.2). Finally, we evaluate the air–sea CO_2 exchanges and assess the interannual variability (Section 3.3).

2. Material and methods

Transects in the EnC have been carried out in two periods during the spring and another two during autumn: early spring (7th March–12th April, 2003), late spring (9th May–9th June, 2003), autumn 2003 (26th–29th September) and autumn 2004 (5th–22th November) with the following number of tracks per period: 11, 9, 2 and 4, respectively. All cruises were performed on board of two ships of opportunity from Flota Suardíaz Company (RO-RO L'Audace and RO-RO Surprise) following the two different commercial routes of the vessels: northern and southern (Fig. 1).

Underway seawater molar fraction of CO_2 (xCO_2^{sw}), atmospheric molar fraction of CO_2 (xCO_2^{atm}), sea surface salinity (SSS), temperature (SST) and chlorophyll (Chl*a*) were measured using an autonomous home-made equipment, a SeaBird thermosalinometer (SBE-45-MicroTSG) and a WETLabs fluorometer, respectively. Seawater was taken from the ship's cooling water supply at a depth of 3 m, pumped at a high flow rate in order to reduce warming across the pipe.

The xCO_2 was measured with a non-dispersive infrared gas analyzer (Licor®, LI-6262). The equipment was calibrated at the beginning and at the end of each transit (26 h per transit) using two gas standards of CO_2: a synthetic free-CO_2 air and a 375 ppmv CO_2 standard in synthetic air, certified by Instituto Meteorológico Nacional (Izaña, Canary Islands). The fCO_2^{sw} was calculated from xCO_2^{sw} as described in DOE (1994) and the temperature shift was accounted for and corrected using the empirical equation proposed by Takahashi et al. (1993). The temperature difference between the ship's sea inlet and the engine room was usually around 0.4 °C. The data was logged with a 1 min frequency, and subsequently a 5 min filtered average is calculated and outliers are removed using a two standard deviation (σ) limit criterion.

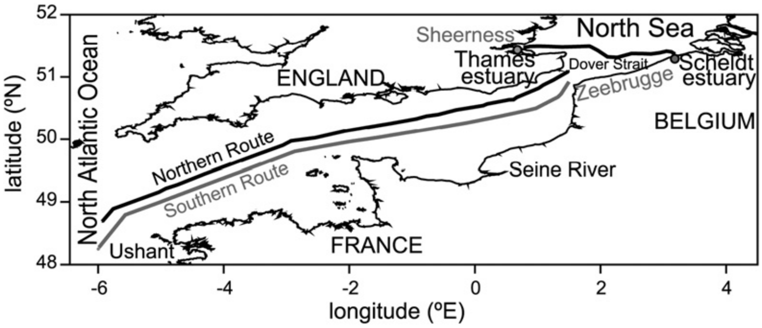

Fig. 1. Map of the investigated area showing the typical northern (black line) and southern (grey line) route covered by the ships of opportunity along the EC and SB.

Together with the xCO_2^{atm} measured on board, another xCO_2^{atm} data set was obtained from Mace Head (Ireland, 53.55°N 9.15°W) meteorological station, which belongs to the air sampling network of NOAA/ESRL Global Monitoring Division. To convert the xCO_2^{atm} to fCO_2^{atm}, the water vapour pressure (pH_2O, in atm) was calculated from in situ temperature (T_{is}, in °C) according to Cooper et al. (1998). A 0.3% decrease between pCO_2^{atm} and fCO_2^{atm} (Weiss, 1974) is assumed to be enough to consider this procedure sufficiently accurate (Olsen et al., 2004).

$$pCO_2^{atm} = xCO_2^{atm} \cdot (p_{atm} - pH_2O)$$

where

$$pH_2O = 0.981 \cdot \exp(14.32602 - (5306.83/(273.15 + T_{is})))$$

To estimate the consistence of the continuous fCO_2^{sw} measurements, the fCO_2^{sw} was computed from the pH and alkalinity using the constants given by Lueker et al. (2000). The pH was determined using a spectrophotometric method according to Clayton and Byrne (1993), and an automatic potentiometric titration (Pérez and Fraga, 1987) was used to estimate the alkalinity. The comparison between the calculated and in situ fCO_2^{sw} values showed a discrepancy of 0.8 ± 6 μatm, comparable to those given by Kortzinger et al. (2000). On the other hand, the chlorophyll concentration was calibrated from GF/F filtered samples and analyzed with the fluorometric method of Yentsch and Menzel (1963), showing an accuracy of ±0.05 mg m^{-3}.

The carbon flux between the atmosphere and the ocean, F (mmol m^{-2} day^{-1}), was calculated using the following equation:

$$F = 0.24kS(fCO_2^{sw} - fCO_2^{atm})$$

where k (cm h^{-1}) is the gas transfer velocity calculated using the Wanninkhof (1992) coefficients for short-term winds. The wind speed was obtained from the Physical Oceanography Distributed Active Archive Center of the Jet Propulsion Laboratory (http://podaac.jpl.nasa.gov) and was measured by the QuikSCAT satellite with temporal and spatial resolutions of 0.25° and 12 h. The wind speed vector was selected from the orbital pass nearest to the measurements, taking spatial proximity as a criterion. Seawater CO_2 solubility (S, mmol m^{-3}·atm^{-1}) was calculated from Weiss (1974) and the constant 0.24 is a unit conversion factor.

3. Results and discussion

3.1. Spatial and temporal variability

3.1.1. Longitudinal variability

The most representative transects for each sampling period performed along the EnC and SB (Fig. 1) are shown in Fig. 2. Considering the division proposed by Reid et al. (1993) according to oceanographic characteristics, the EnC was separated into Western Channel (WC; from 5.2°W to 3.5°W) and Eastern Channel (EC; from 3.5°W to 1.5°E). SB (east of 1.5°E) has been also considered, and is subsequently divided into three regions: the Central Region of Southern Bight (CSB), Scheldt Plume (SP) and Thames Plume (TP). The Armorican Shelf is included as well in the description as a transition region between the oceanic waters of the North Atlantic Ocean and the EnC.

3.1.1.1. Western Channel and Armorican Shelf. The WC is characterized for being the entrance of warmer and saltier waters coming from North Atlantic Ocean into the North Sea (Pingree and Maddock, 1977; Salomon and Breton, 1993). From March to May, the SST decreases eastwards about 1–2 °C, indicating the presence of warmer waters in the WC (Fig. 2a–c). From May to November, the decreasing SSS also shows the eastward dilution of North Atlantic waters (Fig. 2c–f). During the early spring (Fig. 2a, b), a low salinity intrusion appearing in the vicinity of Ushant (48.5°N, 5.1°W) reaching the lowest values in April 2003 (34.1 psu) modifies the expected trend. According to Kelly Gerreyn et al. (2006), the low saline water reaches the Armorican Shelf by advection from Atlantic French Rivers, mainly the Loire and Gironde rivers. In fact, the presence of low SSS water is concomitant with low values of fCO_2^{sw} (~292 μatm, Fig. 2b). In April, there is an entrance of low SSS and fCO_2^{sw} waters containing Chl*a* values of 1.5 mg m^{-3}. In June (Fig. 2d), the entry of saltier waters from the North Atlantic provokes an SSS front around −5°E that generates the observed Chl*a* maximum (3.6 mg m^{-3}), with fCO_2^{sw} values of about 290 μatm. Consequently, the more undersaturated waters in fCO_2^{sw} are located in the west boundary of the WC, with a homogeneous spatial distribution pattern. On the contrary, the observed maxima of fCO_2^{sw} and SST (~425 μatm, ~17.1 °C, Fig. 2e) are reached between 4.0°W and 4.5°W during September. According to the thermodynamic control over fCO_2^{sw} reported by Takahashi et al. (1993), only about 45% of the observed increment corresponding to fCO_2^{sw} maximum can be attributed to SST. Therefore, other processes such as the

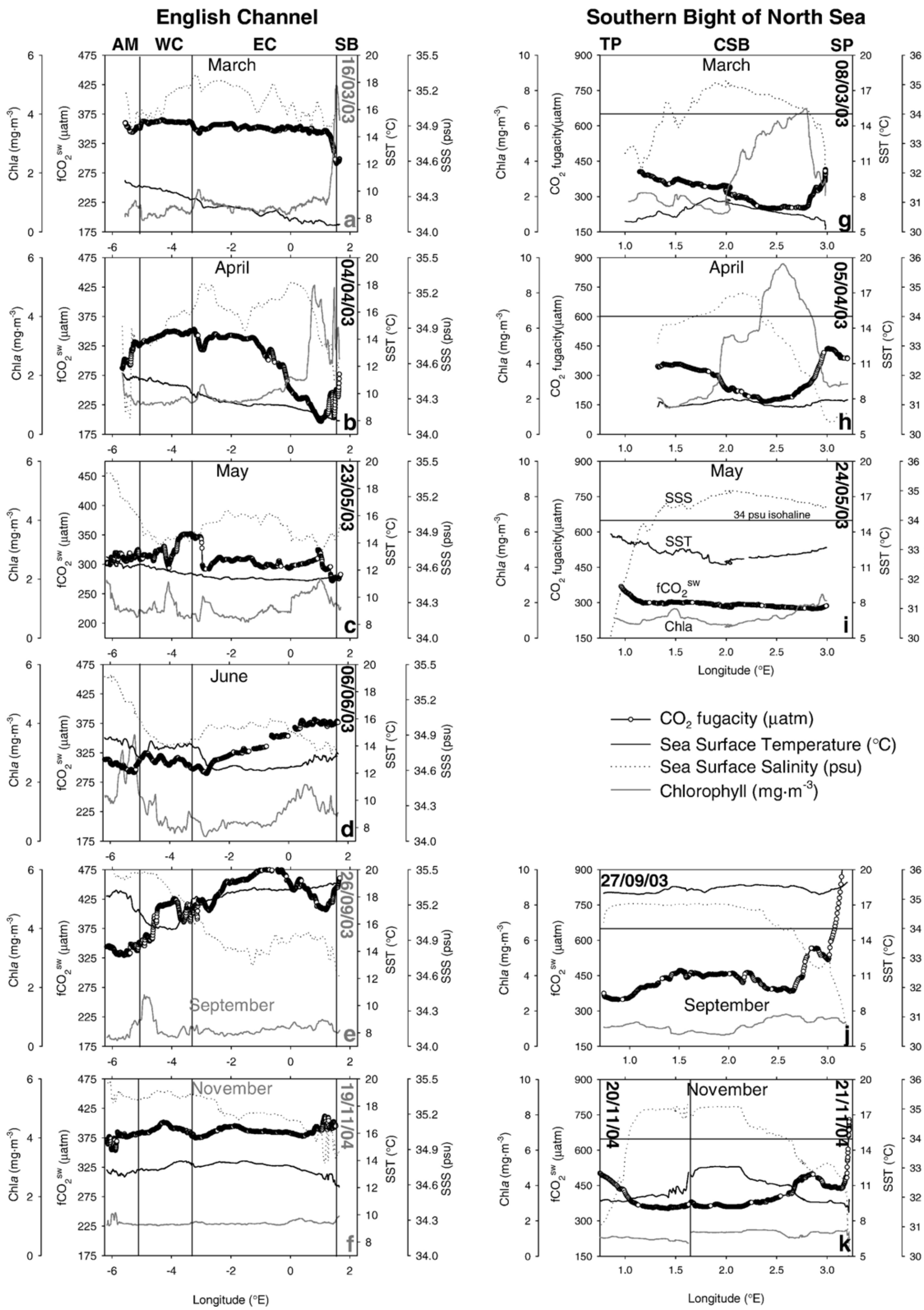

Fig. 2. Distribution of seawater CO_2 fugacity (fCO_2^{sw}), sea surface temperature (SST), sea surface salinity (SSS) and chlorophyll concentration (Chl*a*) along the performed transects in the EC (left panels) and Southern Bight (right panels) at the detailed dates (black date: northern routes and grey date: southern routes). Vertical lines divide the hydrological recognized regions: AM (Armorican Shelf), WC (Western Channel), EC (Eastern Channel), CSB (Central Region of Southern Bight), TP (Thames Plume) and SP (Scheldt Plume).

remineralization of organic matter are likely to be affecting the fCO_2^{sw} distribution.

3.1.1.2. Eastern Channel. In the EC, the water column is permanently well-mixed and receives the majority of the freshwater discharged in the Channel (Reid et al., 1993). The relative SSS minima (Fig. 2a–f) were found close to the mouth of River Seine (~1.5°W) ranging from 34.68 psu in September to 35.14 psu in November (Fig. 2a–f). The absolute SSS minima (~34.6 psu; Fig. 2b, e) were located near to the Dover Strait (~1.5°E), where French river discharges form the "coastal river" (Brylinski et al., 1996) due to the eastward narrowing of the Channel. Along the EC, the SST decreases eastward about 2 °C during early spring and autumn and increases between 2 and 4°C in June and September (Fig. 2), denoting a higher seasonal SST variation of the "coastal rivers" compared to oceanic waters.

The highest values of Chl*a*, ranging from 2 to 5 mg m^{-3}, were also found in the EC close to the SB (Fig. 2a–d) where the lowest fCO_2^{sw} values (lower than 300 µatm) are also located. The maximum Chl*a* value of 7.3 mg m^{-3} during 22nd March (not shown) turned the Dover Strait into the more fCO_2^{sw} undersaturated region of the EC with values around 250 µatm. The annual maximum of fCO_2^{sw} (475 µatm) is linked to water discharges from the River Seine, recorded during the warmest cruise of the sampling periods (19 °C; Fig. 2e). Additionally, close to Dover Strait the spatial variability of fCO_2^{sw} is inversely correlated with SSS (Fig. 2a–f).

3.1.1.3. Southern Bight of North Sea. The SB is a complex area of the North Sea that receives important continental inputs and water fluxes from the North Atlantic Ocean through the EnC. Following Borges and Frankignoulle (2002) the 34 isohaline was used to discriminate between oceanic waters located in the CSB and continental waters of the TP and the SP. In autumn, the estuarine plumes have a strong influence on the fCO_2^{sw}, generating strong longitudinal gradients (Fig. 2j, k). In the proximity of the Scheldt estuary, the lowest SSS coincides with the highest fCO_2^{sw} values, namely, 1470 µatm at 29.91 psu in September (Fig. 2j) and 906 µatm at 29.03 psu in November (Fig. 2k). In March and April, Chl*a* concentrations along the SB are also linked to the estuarine plumes, reaching outstanding values above 7 mg m^{-3} (Fig. 2g, h). This high Chl*a* also accentuates the longitudinal fCO_2^{sw} variation in the SB, leading to fCO_2^{sw} values associated with the SP lower than 200 µatm (Fig. 2g, h). In the TP, higher fCO_2^{sw} and lower Chl*a* values are found, probably due to the reduced nutrient supply and the high turbulence of English waters (Hoch and Ménesguen, 1997).

3.1.2. Latitudinal variability in the English Channel

Consecutive transects along the EnC were equally separated 10–13 miles latitudinal-wise and sampled every 2–3 days. In spite of this, significant differences in fCO_2^{sw}, Chl*a* and SSS were found between consecutive samples. The variability of the latitudinal fCO_2^{sw} differences is lower in the WC (5±7 µatm) than in the EC (−2±26 µatm) throughout the year. During the spring, northern transects generally displayed higher values of fCO_2^{sw} along the EC, whereas during autumn the opposite occurred. The observed latitudinal gradients of SST and fCO_2^{sw} show a negligible correlation, opposite to what Borges and Frankignoulle (2003) had suggested. Nevertheless, the latitudinal changes of fCO_2^{sw} notably correlate with SSS ($r=-0.88$) and, unexpectedly, positively correlate with Chl*a* ($r=0.85$). In early spring, the waters in the Southern area are 0.03±0.02 saltier and 17±7 µatm lower in fCO_2^{sw} than in the North. During late spring and autumn the opposite occurred, being the SSS and fCO_2^{sw} differences −0.05±0.02 and 27±22 µatm, respectively. Therefore the inverse salinity control on fCO_2^{sw} in the EnC is associated with seawater inputs from the North Atlantic Ocean and continental discharges, especially, close to Dover Strait (Fig. 2). This is due to the strong effect exerted by continental discharges introducing high fCO_2^{sw} and moderate Chl*a* values, thus provoking an unpredictably positive correlation between them. It is the first time that the latitudinal fCO_2^{sw} variations are found to be inversely correlated with SSS in the EnC.

3.1.3. Temporal variability

In order to describe the seasonal and short-term variability in the EnC and SB, the measured properties were averaged for every cruise in the separated regions (Fig. 3). Table 1 shows the minima and maxima of these averaged variables and the air–sea CO_2 exchanges, including the Julian day when the extreme values were recorded.

3.1.3.1. English Channel. The left panel in Fig. 3 shows the annual cycle of the air–sea fCO_2 gradient (ΔfCO_2), Chl*a*, SST and SSS in the WC and EC. Seasonal variability of the ΔfCO_2, Chl*a* and SST gathered by Borges and Frankignoulle (2003) (hereinafter, B&F) were superimposed in the figure. The B&F profiles were obtained from cruises performed during the 1990s and were averaged from 5.2°W to 1.5°E.

During spring, surface waters show strong fCO_2 undersaturation (Fig. 3a), reaching the lowest ΔfCO_2 in

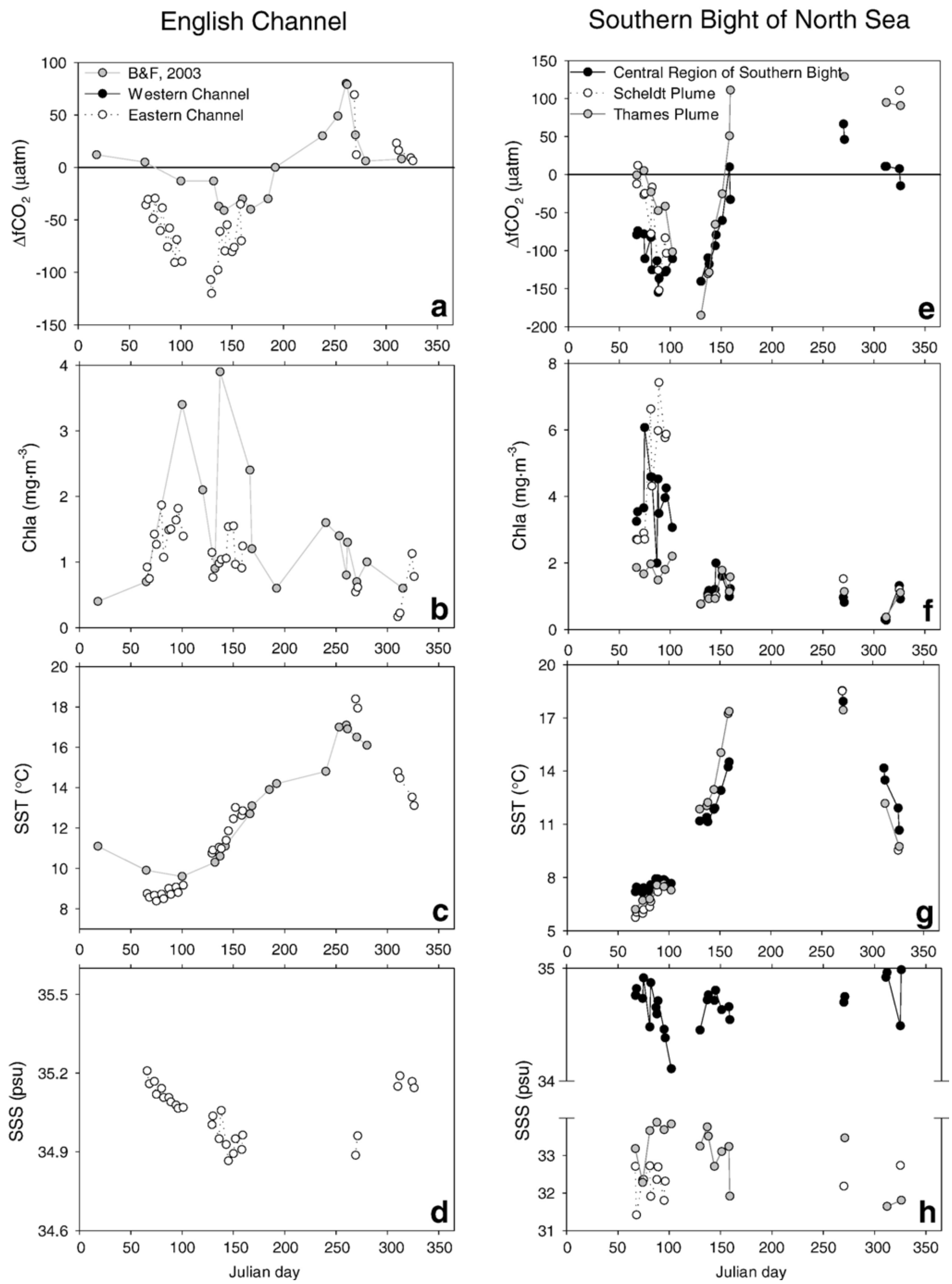

Fig. 3. Seasonal variability of average values of air–sea fCO_2 gradient (ΔfCO_2) (µatm), chlorophyll (mg m^{-3}), temperature (°C) and salinity (psu) measured in the WC and Eastern Channel (left panels) and the Central Region of Southern Bight, SP and TP (right panels). Seasonal cycles of air–sea fCO_2 gradient, chlorophyll and temperature in the EC (from 1.5°E and 5.2°W) reported by Borges and Frankignoulle (2003) are drawn in the left panel.

May (−83 µatm in the west and −120 µatm in the east). The fCO_2^{sw} reported by B&F is systematically less undersaturated than the one shown here. The average differences in fCO_2^{sw} between B&F and our distributions are 32±12 and 50±27 µatm in the WC and EC, respectively. As B&F showed, the highest Chl*a* values are recorded in spring (2±1 mg m^{-3} in WC and 1.3±0.2 mg m^{-3} in EC). However, they recorded higher Chl*a* concentrations than the ones shown here (Fig. 3b). B&F reported slightly lower SSS values suggesting a higher influence of the "coastal river", where the maximum of Chl*a* is located during spring (Brunet et al., 1992). As

Table 1
Minimum and maximum average of seawater CO_2 fugacity, chlorophyll concentration, sea surface temperature, sea surface salinity and air–sea CO_2 flux in the Western Channel (WC), Eastern Channel (EC), Central Region of Southern Bight (CSB), Thames Plume (TP) and Scheldt Plume (SP) measured at the specific date (in Julian days)

		Seawater CO_2 fugacity		Chlorophyll		Sea surface temperature		Sea surface salinity		Air–sea CO_2 flux	
		μatm	Date	mg m^{-3}	Date	°C	Date	psu	Date	mmol C · m^{-2} · day^{-1}	Date
WC	Max	394±7	310	1.3±0.2	90	17±1	269	35.43±0.08	269	4±2	324
	Min	297±17	131	0.37±0.06	66	10.3±0.4	76	34.8±0.3	87	−12±6	157
EC	Max	439±24	269	2±1	80	18.4±0.4	269	35.21±0.07	66	6±3	269
	Min	260±17	130	0.22±0.05	309	8.4±0.6	75	34.87±0.03	145	−13±3	136
TP	Max	499±37	271	2.2±0.2	102	17.44±0.2	271	33.9±0.1	88	39±12	326
	Min	196±5	130	0.37±0.02	312	6.2±0.3	67	32±2	312	−20±7	138
SP	Max	636±283	270	7±2	81	18.5±0.2	270	33±1	325	48±27	325
	Min	228±53	89	1.2±0.1	325	5.7±0.4	68	31±2	68	−31±25	96
CSB	Max	436±31	270	6±2	75	18.5±0.4	270	35±0.1	326	10±6	325
	Min	226±40	88	0.30±0.06	312	7.1±0.3	74	34.11±0.04	102	−31±20	67

described in the former epigraph, the effect of the high CO_2 and Chl*a* continental waters would explain the differences between the two data sets. In this sense, the intensity of coastal rivers would generate interannual differences which manifest on the B&F and ECO data sets. Besides, it can be observed that the fCO_2^{sw} and SST minima are reached about 1 month earlier than those reported by B&F (Fig. 3).

In spite of the lack of data in the summer period, the ΔfCO_2 maximum (~69 μatm) obtained in September is very close to the seasonal maximum reported by B&F. On the other hand, ΔfCO_2, chlorophyll and SST values are quite consistent with B&F gathered data set during autumn along the EnC.

3.1.3.2. Southern Bight of the North Sea. The seasonal variation of ΔfCO_2, Chl*a*, SST and SSS is shown in the right panel of Fig. 3. During early spring, the CSB shows strong CO_2 undersaturation (−150 μatm, Fig. 3e). The SP and TP have also been classified as CO_2 undersaturation zones for this period, yet during the first surveys, except for the CSB, the measured fCO_2^{sw} in these two regions was practically in equilibrium with the atmosphere. At this same period, the Chl*a* reached the annual maxima in every considered region (Fig. 3f; Table 1). The highest Chl*a* measurements are found in the SP (7±2 mg m^{-3}).

It is worth highlighting the fCO_2^{sw} increase of 150 μatm reaching the atmospheric equilibrium in the CSB during late spring. The TP also shows an increase of 296 μatm attaining a noticeable CO_2 oversaturation of 111 μatm in only 30 days. The SST effect on the fCO_2^{sw} increase in the TP region is evident and can be quantified. An SST increase of 6.5 °C over 30 days would yield an fCO_2^{sw} increase of 60 μatm according to Takahashi et al. (1993), that is notably lower than the recorded value of 296 μatm. Therefore, besides the temperature control representing only one fifth of the observed increment of fCO_2^{sw}, the input of continental waters together with the SSS minimum (Fig. 3h) may also be having an effect. Remineralization could be also involved in this fCO_2^{sw} increase since it also depends on temperature or carbonate production (Migné et al., 1998).

In autumn the entire Southern Bight was oversaturated with CO_2, reaching the maximum values of the seasonal cycle during September. The SP and TP regions display very high fCO_2^{sw} values of 636±283 and 499±37 μatm, respectively (Table 1). On the other hand, the CSB shows an annual maximum of 436±31 μatm, but this value progressively decreases to a value close to the atmospheric equilibrium in November, unlike in the riverine plume cases. During this period, the Chl*a* concentration displays the lowest values (Fig. 3f; Table 1) forming the annual Chl*a* minimum (0.30±0.06 mg m^{-3}) in the CSB.

Along the SB, the effect of continental waters increases the amplitude of the seasonal fCO_2^{sw}, SST and even Chl*a* ranges. The broadest amplitudes of these averaged variables (12.9 °C, 408 μatm and 5.8 mg m^{-3}) were registered in the SP and displayed a good deal of freshwater inputs (Fig. 3h). The CSB (11.4 °C, 210 μatm and 5.7 mg m^{-3}) and the TP (11.2 °C, 303 μatm and 1.8 mg m^{-3}) also showed a wide variability, consistent with the average SSS (Fig. 3h). In summary, waters with low SSS show broad fCO_2^{sw} amplitudes.

3.2. The role of biology and the temperature effect on fCO_2^{sw}

With the aim of evaluating the biological control over fCO_2^{sw} in the EnC and the SB, Chl*a*–fCO_2^{sw}

Table 2
Coefficients from significant linear regressions performed by plotting 5 min filtered averages of seawater CO_2 fugacity (μatm) and chlorophyll concentration (mg m^{-3}) in the Western Channel (WC), EC (Eastern Channel), TP (Thames Plume), SP (Scheldt Plume) and CSB (Central Region of Southern Bight) according to equation: $fCO_2 = fCO_{2o} + b \cdot \mathrm{Chl}a$

	7th March–12th April 2003				9th May–9th June 2003				26th–29th September 2003				5th–22nd November 2004			
	fCO_{2o}	b	n	fCO_2	fCO_{2o}	b	n	fCO_2	fCO_{2o}	b	n	fCO_2	fCO_{2o}	b	n	fCO_2
			r	Chl*a*			r	Chl*a*			r	Chl*a*			r	Chl*a*
WC	369	−24	880	346±16	315	−4	734	311±19			205	395±28	400	−14	165	386±11
			0.55	1.0±0.4			0.11	0.9±0.4				0.6±0.3			0.59	1.0±0.5
EC	369	−30	1348	323±41			1093	301±30	479	−108	232	415±34	399	−11	466	391±8
			0.76	1.5±1.0				1.1±0.4			0.41	0.6±0.1			0.57	0.8±0.4
TP	386	−16	103	356±41	212	121	84	376±97							17	469±47
			0.21	1.9±0.5			0.56	1.4±0.5								1.0±0.4
SP	458	−26	307	317±83	1364	−285	28	811±156	2441	−1178	87	696±348			42	507±91
			0.85	5±3			0.98	2.0±0.6			0.67	1.5±0.2				1.5±0.2
CSB	337	−15	364	278±48	273	21	347	300±45	484	−61	116	427±33	389	−6	196	382±15
			0.73	4±2			0.23	1.3±0.5			0.54	0.9±0.3			0.20	1.0±0.5

fCO_{2o} is the intercept for the zero chlorophyll, *b* is the slope of the linear regression, *n* is the number of data, *r* is the regression coefficient and fCO_2 and Chl*a* are the average values of seawater CO_2 fugacity (μatm) and chlorophyll concentration (mg m^{-3}), respectively, in each indicated period for the every separated region.

relationships are studied in every region during the four sampling periods (Table 2). According to Watson et al. (1991) and Frankignoulle et al. (1996) the recent phytoplankton bloom is characterized by a slope around 17 μatm·(mg $m^{-3})^{-1}$ and an fCO_2^{sw} intercept around the fCO_2^{atm}. On the other hand, late stages of the bloom yield a lower slope and intercept caused by the CO_2 equilibration delay after Chl*a* disappears due to sedimentation and grazing. Considering the data from Mace Head meteorological station (Ireland), the fCO_2^{atm} was 367±3 μatm for 2003.

During spring, the Chl*a*–fCO_2^{sw} relationships obtained for the WC and EC and even for the TP are close to those accepted for a recent phytoplankton bloom (Table 2). The Chl*a*–fCO_2^{sw} relationships obtained for the CSB during spring and for the WC in late spring show low slopes and intercepts, indicating a late stage of the bloom. However, the *y*-intercept obtained during spring for the SP is higher than the fCO_2^{atm}, probably due to the contribution from continental waters. On the other hand, during autumn, the *y*-intercept values (389–400 μatm) obtained for the EC and CSB are also higher than the fCO_2^{atm}, most likely because of the summer heating and slow equilibration rates of the oceanic waters. The slopes of the Chl*a*–fCO_2^{sw} relationships are comparable to those expected throughout the bloom, suggesting a significant influence of the autumn bloom. During late spring and early autumn, in spite of the significant correlations obtained for CSB, the slopes have no biological meaning since they are quite negative or even positive. It is most likely that the influence of moderate chlorophyll and high fCO_2^{sw} continental waters are responsible for these bizarre slopes.

Following Takahashi et al. (2002), the temperature control over fCO_2^{sw} by the SST variation can be removed using the equation:

$$fCO_2^{sw}{}_{\mathrm{SSTm}} = fCO_2^{sw}\exp[0.0423(\mathrm{SST_{mean}} - \mathrm{SST})]$$

where the $\mathrm{SST_{mean}}$ and $fCO_2^{sw}{}_{\mathrm{SSTm}}$ stand for the annual mean SST and the $fCO_2^{sw}{}_{\mathrm{SSTm}}$ normalized to the $\mathrm{SST_{mean}}$, respectively. In order to evaluate the temperature influence on the fCO_2^{sw} alone, the effect of the difference between SST and $\mathrm{SST_{mean}}$ on the annual mean of fCO_2^{sw} ($fCO_2^{sw}{}_{\mathrm{mean}}$) is computed according to the equation:

$$^{SST}fCO_2^{sw}{}_{\mathrm{mean}} = fCO_2^{sw}{}_{\mathrm{mean}}\exp[0.0423(\mathrm{SST} - \mathrm{SST_{mean}})]$$

where $^{\mathrm{SST}}fCO_2^{sw}{}_{\mathrm{mean}}$ stands for the annual $fCO_2^{sw}{}_{\mathrm{mean}}$ at the observed SST. The values of $\mathrm{SST_{mean}}$ and $fCO_2^{sw}{}_{\mathrm{mean}}$ are given in Table 3. The amplitudes of the seasonal cycle for SST (Table 1, Fig. 3c, g) are 6.7, 10 and 11.4 °C in the WC, EC, and CSB respectively. So, the wider SST

Table 3
Annual mean of SST (°C) and fCO_2^{sw} (μatm) along the English Channel and Central Region of Southern Bight computed to estimate the biological and temperature control on the fCO_2^{sw} distribution

	Western Channel	Eastern Channel	Southern Bight
$\mathrm{SST_{mean}}$	14.02	13.66	13.74
$fCO_2^{sw}{}_{\mathrm{mean}}$	349	352	351
$\Delta fCO_2^{sw}{}_{\mathrm{bio}}$	121	146	147
$\Delta fCO_2^{sw}{}_{\mathrm{temp}}$	98	148	164
Ratio	0.8	1.0	1.1

Net biological utilization ($\Delta fCO_{2\mathrm{bio}}^{sw}$, μatm) and the temperature effect ($\Delta fCO_2^{sw}{}_{\mathrm{temp}}$, μatm) are included with the ratio between the biology and temperature effect.

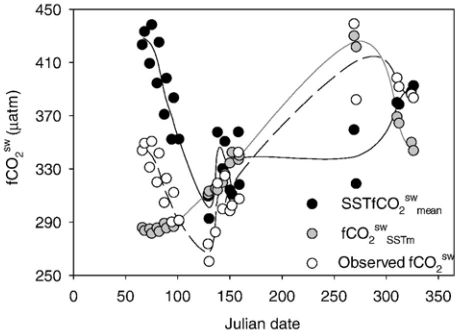

Fig. 4. The averaged values of observed fCO_2^{sw} (white circles and dash line), fCO_2^{sw} at the mean water temperature of 13.66°C ($fCO_2^{sw}{}_{SSTm}$, black circles and black line) and the annual mean fCO_2^{sw} value corrected for changes in temperature ($^{SST}fCO_2^{sw}{}_{mean}$, grey circles and grey line) for each ECO transect in the Eastern Channel.

amplitude measured in the CSB produces a seasonal shift of 164 µatm, whereas the EC and WC are 148 and 98 µatm, respectively (Table 3).

For the EC the effect of SST and biology over fCO_2^{sw} is shown in Fig. 4. The maximum values of $fCO_2^{sw}{}_{SSTm}$ are observed in early spring. Within a short period of time the $fCO_2^{sw}{}_{SSTm}$ minimum is reached, and it keeps nearly constant from late spring to early autumn. Later in autumn, the heterotrophic processes increase these $fCO_2^{sw}{}_{SSTm}$ values.

The difference between the maximum (pre-bloom) and minimum (end of the bloom) of $fCO_2^{sw}{}_{SSTm}$ takes into account the net biological effect on fCO_2 seasonal cycle ($\Delta fCO_2^{sw}{}_{bio}$). The EC and the CSB showed similar net biological effects of 146 and 147 µatm, respectively (Table 3). These net biological signals are stronger than the newer ones of 130 µatm in the SB, reported by Thomas et al. (2005). The WC shows a weaker net biological effect (121 µatm). The three regions are within the range of net biological effect on fCO_2^{sw} of 120 µatm proposed by Takahashi et al. (2002) at these latitudes in the North Atlantic Ocean. The SST and the net biological effects were very similar in magnitude. The net biological effect mainly dominates in spring whereas the SST especially controls the fCO_2^{sw} in summer (Table 3).

3.3. Air–sea CO_2 exchanges

The air–sea CO_2 fluxes were computed using xCO_2^{atm} from Mace Head (Ireland) meteorological station, where several data selection criteria are applied to obtain uncontaminated xCO_2^{atm} measurements. These air–sea CO_2 fluxes are described in two regions: SB and EnC.

3.3.1. Southern Bight of North Sea

The SB behaves as a CO_2 sink during spring, especially in the CSB where averaged CO_2 recorded values amount up to -11 ± 11 mmol m^{-2} day^{-1}. In comparison, the TP presents a smaller uptake capacity of -4 ± 9 mmol m^{-2} day^{-1} at the same period. The CO_2 uptake value of -11 ± 12 mmol m^{-2} day^{-1} obtained for the SP is only calculated for the early spring bloom. An accentuated CO_2 source role occurred during autumn, with averaged CO_2 release values for the separated regions CSB, TP and SP of 4 ± 3, 35 ± 20 and 24 ± 15 mmol $m^{-2}\cdot day^{-1}$, respectively.

The air–sea CO_2 exchanges in the SP and TP proximal areas suggest a tendency to behave as CO_2 sources (Smith and Mackenzie, 1987; Frankignoulle et al., 1996; Gattuso et al., 1998; Cai and Wang, 1998; Cai et al., 1999, 2000; Raymond et al., 2000). On the contrary, the CSB displays a trend to net CO_2 uptake as expected in the distal regions (Boehme et al., 1998; Tsunogai et al., 1999; Frankignoulle and Borges, 2001; Borges and Frankignoulle, 2002).

3.3.2. English Channel

In the EnC the ΔfCO_2 pattern clearly discriminates between two periods (Fig. 3a): from March to June the area acts as a CO_2 sink, and from August to January as a CO_2 source. From March to June, the computed air–sea

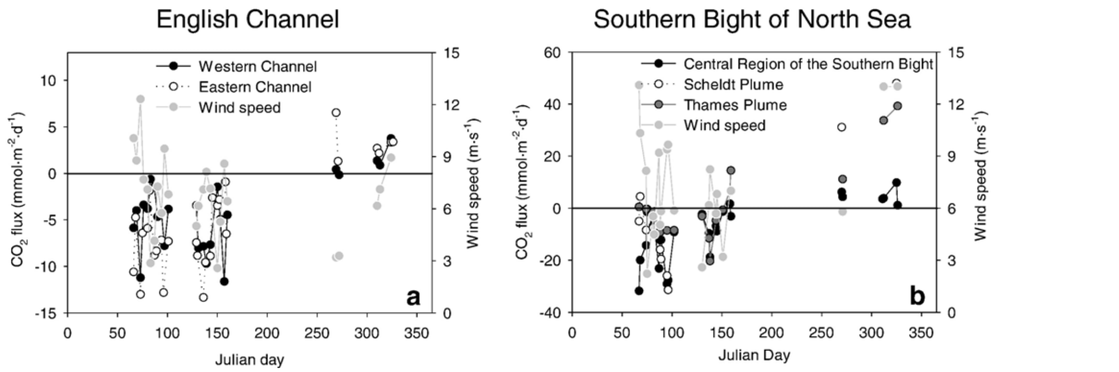

Fig. 5. Seasonal variability of average air–sea CO_2 flux (mmol·m^{-2} day^{-1}) in the (a) WC and Eastern Channel and in the (b) Central Region of Southern Bight, SP and Thames Plume. Average remote wind speed measured from QuikSCAT sensor (m s^{-1}) in the EC (a) and in the SB (b).

CO_2 fluxes (Fig. 5a) show the expected strong CO_2 uptake both in the WC (-7 ± 4 mmol m^{-2} day^{-1}) and EC (-11 ± 7 mmol m^{-2} day^{-1}). These intense absorption of atmospheric CO_2 during the spring were close to -6.5 mmol m^{-2} day^{-1}, found by Wang et al. (2000) for the East China Sea. During autumn, the CO_2 outgassing obtained at the end of September and November was in average of 1 ± 2 and 3 ± 2 mmol m^{-2} day^{-1} for the WC and EC, respectively. In the EnC, B&F computed very low CO_2 fluxes during March and April (-1 ± 1 mmol m^{-2} day^{-1}) meanwhile the uptake was intensified ($-4\pm$ 2 mmol m^{-2} day^{-1}) during the May and June. These same authors have additionally estimated a CO_2 outgas of $2\pm$ 1 mmol m^{-2} day^{-1} during autumn in this region.

From the ECO cruises, the CO_2 seasonal cycle at annual scale cannot be obtained due to the gaps in the sampling coverage. B&F were able to complete a seasonal cycle from data gathered in different years, and classified the EnC as a weak CO_2 source. They provided a net annual air–sea flux of 1.3 ± 1.7 mmol m^{-2} day^{-1} computed with the exchange coefficient of Nightingale et al. (2000) and the daily geostrophic wind speeds from 1995 to 1999. Using the seasonal air–sea pCO_2 gradient proposed by B&F, Wanninkhof's transfer velocity and recent remote sensing measurements of wind speed obtained by QuikSCAT satellite from 2000 to 2004, the recalculated annual CO_2 flux is 0.8 ± 1.7 mmol m^{-2} day^{-1}. This is not statistically different to the one previously estimated by B&F.

Taking into account the important ΔfCO_2 discrepancies found during spring, a revised CO_2 seasonal cycle was obtained updating the B&F data set with the ECO cruises. The estimated annual CO_2 exchange of $-1.0\pm$ 3.2. mmol m^{-2} day^{-1} places the EnC as a slight CO_2 sink. To evaluate the anthropogenic influence of xCO_2^{atm} on the CO_2 flux following B&F, the xCO_2^{atm} difference between ship-board measurements and Mace Head's (Ireland) was estimated in 4 ± 8 ppm and 7 ± 9 ppm in the EC and CSB, respectively while the WC is negligible. Contemplating this anthropogenic effect, the CO_2 exchange in the EnC rises to -1.3 ± 3.2 mmol $m^{-2}\cdot day^{-1}$.

According to the seasonal cycles proposed by either B&F or that modified with ECO observations, the EnC seems to behave as a neutral area of CO_2 exchange at an annual scale. The average difference of the CO_2 exchange between both ΔfCO_2 seasonal cycles was statistically estimated at an annual scale by means of a paired-sample *t*-test. Results indicate that the two data sets significantly differ from each other to a 95% degree of confidence by a mean disagreement of -2.0 mmol m^{-2} day^{-1} with a standard error of the mean of 0.2 mmol m^{-2} day^{-1}. This different behaviour derives from the ΔfCO_2 observed discrepancies during the spring. In the epigraph "Latitudinal variability in the English Channel", an inverse correlation between the latitudinal fCO_2^{sw} and SSS variations was described. This very same covariation is also observed in the SB where the riverine plumes advect high fCO_2 water inputs into a more oceanic environment with lower fCO_2 values coming from Bay of Biscay (Frankignoulle and Borges, 2001). The balance between the spreading of both oceanic and riverine waters in the EnC affects decisively the annual average of CO_2 exchange. The interannual variations in SSS levels in the EnC and SB caused by the different water mass and the meteorological parameters have been reported by Becker et al. (1993). These variations have been associated to North Atlantic Oscillation (NAO) at a decadal timescale, which relates directly with river discharges and water mass salinities (Perez et al., 1995; González-Pola et al., 2005). Therefore, the role of the EnC as a sink/source of CO_2 can be finally determined from the interannual climatological conditions, since the biological and temperature effects balance out in an annual basis.

4. Conclusions

The biological and temperature effect appears to equally control the seasonal cycle of fCO_2^{sw} along EnC and SB. Good correlations between fCO_2^{sw} and Chl*a* were found during spring and are in good agreement with those obtained by Watson et al. (1991) for the North Atlantic. The thermodynamic control on fCO_2^{sw} predominates from late spring to autumn, this being opposite and similar in magnitude to the net biological effect.

The seasonal fCO_2^{sw} cycles shows a spatial variability modulated by the water mixing between continental inputs and North Atlantic Waters and produces strong latitudinal/longitudinal fCO_2^{sw} gradients.

The interannual variability of fCO_2 here described would hinder the obtaining of an appropriate seasonal cycle from measurements obtained in different years (B&F). Furthermore, the strong spatial variability in the EnC suggests that there is a need for developing intensive sampling cruises if the interannual fCO_2^{sw} variability is to be constrained. Ships of opportunity hence become decisive tools in this regard, since they could provide a handful of exhaustive and accurate measurements.

Acknowledgements

This work was developed and funded within the ECO project (MCyT REN2002-00503/MAR) and from

European Commission (EU FP6 CARBOOCEAN Integrated Project, Contract No. 511176-2). “Diputation de Pontevedra” financed X.A. Padin with a predoctoral grant. We want to especially thank the Captains and crew of *RO-RO L'Audace* and *RO-RO Surprise* together with the management team of Suardiaz Company, for their hospitality and essential help throughout the 2 years. We also express our gratitude to M. Castaño, O. Pereira, F. Alonso, P. Conde and M. Alvarez for their help during ship-board sampling and G. Navarro who kindly provided the remote sensing images processed in the Ocean Color Remote Sensing Service at ICMAN-CSIC. We also thank the NOAA/ESRL Global Monitoring Division for having provided atmospheric CO_2 flask data recorded at Mace Head.

References

Becker, G., Corten, A., Dooley, H., 1993. Recent high salinity in the English Channel/Southern North Sea. ICES Council Meeting C.M., 1992/C6. 11 pp.

Boehme, S.E., Sabine, C.L., Reimers, C.E., 1998. CO_2 fluxes from a coastal transect: a time-series approach. Marine Chemistry 63, 49–67.

Borges, A.V., Frankignoulle, M., 2002. Distribution and air–water exchange of carbon dioxide in the Scheldt plume off Belgian coast. Biogeochemistry 59 (1–2), 41–67.

Borges, A., Frankignoulle, M., 2003. Distribution of surface carbon dioxide and air–sea exchange in the English Channel and adjacent areas. Journal of Geophysical Research 108 (C5), 3140. doi:10.1029/2000JC000571.

Brunet, C., Brylinski, J.M., Frontier, S., 1992. Productivity, photosynthetic pigments and hydrology in the coastal front of the Eastern English Channel. Journal of Plankton Research 14, 1541–1552.

Brylinski, J.M., Brunet, C., Bentley, D., Thoumelin, G., Hilde, D., 1996. Hydrography and phytoplankton biomass in the Eastern English Channel in Spring 1992. Estuarine, Coastal and Shelf Science 43, 507–519.

Cai, W.-J., Dai, M., 2004. Comment on “Enhanced open ocean storage of CO_2 from shelf sea pumping”. Science 206, 1477.

Cai, W.J., Wang, Y., 1998. The chemistry, fluxes, and sources of carbon dioxide in the estuarine waters of the Satilla and Altamaha Rivers, Georgia. Limnology and Oceanography 43 (4), 657–668.

Cai, W.J., Pomeroy, L.R., Moran, M.A., Wang, Y., 1999. Oxygen and carbon dioxide mass balance for the estuarine-intertidal marsh complex of rivers in the southeastern U.S. Limnology and Oceanography 44 (3), 639–649.

Cai, W.-J., Wiebe, W.J., Wang, Y., Sheldom, J.E., 2000. Intertidal marsh as a source of dissolved inorganic carbon and a sink of nitrate in the Santilla River estuarine complex in the Southeastern U.S. Limnology and Oceanography 45, 1743–1752.

Cai, W.-J., Wang, Z.H.A., Wang, Y., 2003. The role of marsh dominated heterotrophic continental margins in transport of CO_2 between the atmosphere, the land–sea interface and the ocean. Geophysical Research Letters 30 (16), 1849. doi:10.1029/2003GL017633.

Chen, C.T.A., Wang, S.L., 1999. Carbon, alkalinity and nutrient budgets on the East Chine Sea continental shelf. Journal of Geophysical Research 104 (C9), 20675–20686.

Clayton, T.D., Byrne, R.H., 1993. Spectrophotometric seawater pH measurements: total hydrogen ion concentration scale calibration of *m*-cresol purple and at-sea results. Deep-Sea Research II 40 (10), 2115–2129.

Cooper, D.J., Watson, A.J., Ling, R.D., 1998. Variation of pCO_2 along a North Atlantic shipping route (U.K. to Caribbean): a year of automated observations. Marine Chemistry 60, 147–164.

DeGrandpre, M.D., Olbu, G.J., Beatty, C.M., Hammar, T.R., 2002. Air–sea CO_2 fluxes on the US Middle Atlantic Bight. Deep-Sea Research II 49 (20), 4355–4367.

DOE, 1994. Handbook of methods for the analysis of various parameters of carbon dioxide in seawater; version 2. In: Dickson, A.G., Goyet, C. (Eds.), ORNL/CDIAC-74.

Fasham, M.J.R., Balino, B.M., Bowles, M.C. (Eds.), 2001. A New Vision of Ocean Biogeochemistry after a Decade of the Joint Global Ocean Flux Study (JGOFS). AMBIO, Special Rep. 10. Royal Swedish Academy of Sciences. Stockholm, Sweden. 31 pp.

Frankignoulle, M., Borges, A.V., 2001. European continental shelf as a significant sink for atmospheric carbon dioxide. Global Biogeochemical Cycles 15 (3), 569–576.

Frankignoulle, M., Bourge, I., Canon, C., Dauby, P., 1996. Distribution of surface seawater partial CO_2 pressure in the English Channel and in the Southern Bight of the North Sea. Continental Shelf Research 16, 381–395.

Gattuso, J.P., Frankignoulle, M., Wollast, R., 1998. Carbon and carbonate metabolism in coastal aquatic ecosystems. Annual Review Ecology Systems 29, 405–434.

González-Pola, C., Lavín, A., Vargas-Yañez, M., 2005. Intense warming and salinity modification of intermediate water masses in the southeastern corner of the Bay of Biscay for the period 1992–2003. Journal of Geophysical Research 110, C05020. doi:10.1029/2004JC002367.

Goyet, C., Millero, F.J., O'Sullivan, D.W., Eischeid, G., McCue, S.J., Bellerby, R.G.J., 1998. Temporal variations of pCO_2 in surface seawater of the Arabian Sea in 1995. Deep-Sea Research I 45, 609–623.

Hoch, T., Ménesguen, A., 1997. Modelling the biogeochemical cycles of elements limiting primary production in the English Channel II. Sensitivity analyses. Marine Ecology Progress Series 146, 189–205.

Ito, R.G., Schneider, B., Thomas, H., 2005. Distribution of surface fCO_2 and air–sea fluxes in the Southwestern subtropical Atlantic and adjacent continental shelf. Journal of Marine System 56, 227–242.

Kelly Gerreyn, B.A., Hydes, D.J., Fernand, L.J., Jegou, A.M., Lazure, P., Puillat, I., García-Soto, C., 2006. Low salinity intrusions in the western English Channel. Continental Shelf Research 26 (11), 1241–1257.

Kortzinger, A., Mintrop, L., Wallace, D.W.R., Johnson, K.M., Neill, C., Tilbrook, B., Towler, P., Inoue, H.Y., Ishii, M., Shaffer, G., Torres Saavedra, R.F., Ohtaki, E., Yamashita, E., Poisson, A., Brunet, C., Schauer, B., Goyet, C., Eischeid, G., 2000. The international at sea intercomparison of fCO_2 systems during the R/V Meteor cruise 36/1 in the North Atlantic Ocean. Marine Chemistry 72, 171–192.

Longhurst, A., Sathyendranath, S., Platt, T., Caverhill, C., 1995. An estimate of global primary production in the ocean from satellite radiometer data. Journal of Plankton Research 17 (6), 1245–1271.

Lueker, T.J., Dickson, A.G., Keeling, C.D., 2000. Ocean pCO_2 calculated from dissolved inorganic carbon, alkalinity, and equations for K1 and K2: validation based on laboratory measurements of CO_2 in gas and seawater at equilibrium. Marine Chemistry 70, 105–119.

Migné, A., Davout, D., Gatusso, J.-P., 1998. Calcium carbonate production of dense population of the brittle star population *Ophiotrix fragilis* (Echinodermata: Ophiuroidea): role in the carbon cycle of a temperate coastal ecosystem. Marine Ecology Progress Series 173, 305–308.

Nightingale, P.D., Liss, P.S., Schlosser, P., 2000. Measurements of air–sea gas transfer during an open ocean algal bloom. Geophysical Research Letters 27, 2117–2120.

Olsen, A., Triñanes, J.A., Wanninkhof, R., 2004. Sea–air flux of CO_2 in the Caribbean Sea estimated using in situ and remote sensing data. Remote Sensing of Environment 89 (3), 309–325.

Pérez, F.F., Fraga, F., 1987. A precise and rapid analytical procedure for alkalinity determination. Marine Chemistry 21, 169–182.

Perez, F.F., Ríos, A.F., King, B.A., Pollard, R.T., 1995. Decadal changes of the theta–*S* relationship of the eastern North Atlantic Central Water. Deep Sea Research I 42, 1849–1864.

Pingree, R., Maddock, L., 1977. Tidal eddies and coastal discharge. Journal of Marine Biology Association UK 57, 869–875.

Raymond, R.A., Bauer, J.E., Cole, J.C., 2000. Atmospheric CO_2 evasion, dissolved inorganic carbon production and net heterotrophy in the York river estuary. Limnology and Oceanography 45, 1707–1717.

Reid, P.C., Auger, C., Chaussepied, M., Burn, M. (Eds.), 1993. The channel, report on sub-region 9, quality status report of the North Sea 1993, 153 pp., UK Dep. of the Environ., Republi. Fr. Minist. De l’Envion., Inst. Fr. De Rech. Pour l’Exploit de la Mer, Brest.

Salomon, J.C., Breton, M., 1993. An atlas of long-term currents in the channel. Oceanologica Acta 16, 439–448.

Smith, S.V., Mackenzie, F.T., 1987. The ocean as a net heterotrophic system: implications from the carbon biogeochemical cycle. Global Biogeochemical Cycles 1 (3), 187–198.

Takahashi, T., Olafsson, J., Goddard, J., Chipman, D.W., Sutherland, S.C., 1993. Seasonal variation of CO_2 and nutrients in the high latitude surface oceans: a comparative study. Global Biogeochemical Cycles 7, 843–878.

Takahashi, T., Sutherland, S.C., Sweeney, C., Poisson, A., Metzl, N., Tilbrook, B., Bates, N.R., Wanninkhof, R., Feely, R.A., Sabine, C.L., Olafsson, J., Nojiri, Y., 2002. Global sea–air CO_2 flux based on climatological surface ocean pCO_2 and seasonal biological and temperature effects. Deep-Sea Research II 49, 1601–1622.

Thomas, H., Schneider, B., 1999. The seasonal cycle of carbon dioxide in the Baltic Sea surface water. Journal of Marine System 22, 53–67.

Thomas, H., Bozec, Y., Elkalay, K., De Baar, H., 2004. Enhanced open ocean storage of CO_2 from shelf sea pumping. Science 304, 1005–1008.

Thomas, H., Bozec, Y., Elkalay, K., De Baar, H.J.W., Borges, A.V., Schiettecatte, L.-S., 2005. Controls of the surface water partial pressure of CO_2 in the North Sea. Biogeosciences 2, 323–334.

Tsunogai, S., Watanabe, S., Sato, T., 1999. Is there a “continental shelf pump” for the absorption of atmospheric CO_2? Tellus 51B, 701–712.

Walsh, J.J., 1988. On the Nature of Continental Shelves. Academic Press, New York. 520 pp.

Walsh, J.J., Rowe, G.T., Iverson, R.L., McRoy, C.P., 1981. Biological export of shelf carbon is a sink of the global CO_2 cycle. Nature 291, 196–201.

Wang, S.L., Chen, C.T.A., Hong, G.H., Chung, C.S., 2000. Carbon dioxide and related parameters in the East China Sea. Continental Shelf Research 20, 525–544.

Wanninkhof, R., 1992. Relationship between wind speed and gas exchange over the ocean. Journal of Geophysical Research 97 (C5), 7373–7382.

Watson, A.J., Robinson, C., Robinson, J.E., Williams, P.J. le B., Fasham, M.J.R., 1991. Spatial variability in the sink for atmospheric carbon dioxide in the North Atlantic. Nature 350, 50–53.

Weiss, R.F., 1974. Carbon dioxide in water and seawater: the solubility of non-ideal gas. Marine Chemistry 2, 203–215.

Yentsch, C.S., Menzel, D.W., 1963. A method for the determination of phytoplankton chlorophyll and phaeophytin by fluorescence. Deep-Sea Research II 10, 221–231.

Zhai, W., Dai, M., Cai, W.-J., Wang, Y., Hong, H., 2005. The partial pressure of carbon dioxide and air–sea fluxes in the northern South China Sea in spring, summer and autumn. Marine Chemistry 96, 87–97.